RESEARCH ON THE ST3 CARBON STEEL CORROSION IN THE PRESENCE OF MICROORGANISMS ISOLATED FROM THE GROUNDWATER AT THE YENISEISKIY SITE

Boldyrev K. A.[1], Safonov A. V.[2], Abramova E. S.[2], Gladkikh N. A.[2], Kryuchkov D. V.[1]

[1]Nuclear Safety Institute of the Russian Academy of Sciences, Moscow, Russia

[2]Federal State Budgetary Institution of Science A. N. Frumkin Institute of Physical Chemistry and Electrochemistry of the Russian Academy of Sciences, Moscow, Russia

Article received on June 24, 2021

The paper presents the experimental study exploring the corrosion of carbon steel St3 samples in the presence of a microbiological community sampled at the Yeniseiskiy site and the microbiota of bentonite clays. Depending on the conditions, an average 3—30-fold increase in the corrosion rate of steel was observed due to the biogenic and biogenic-mediated processes. The maximum steel degradation effect was observed at a temperature of 50 °C in the presence of sulfate ions under conditions being considered optimal for sulfate-reducing bacteria. The developed steel corrosion model was used to determine the activation energy of the aerobic and anaerobic corrosion process.

Keywords: *carbon steel, microbial corrosion, anaerobic corrosion, aerobic corrosion, sulfate-reducing bacteria, geochemical modeling, PHREEQC, radioactive waste.*

Introduction

Various types of bedrock are considered by many countries as potentially suitable for the final disposal of high-level waste: granitoid massif (Finland, Sweden), granite-gneiss formation (the Russian Federation, the Republic of Korea, China), clay formations (France, Belgium), salt formations (USA) [1—3]. The safety strategy in case of deep radioactive waste (RW) disposal facilities assumes maximum RW containment and isolation within the disposal site provided by a multi-barrier safety cascade involving engineered safety barriers (EBS) and the natural environment.

Carbon steel, stainless steel, copper, deoxygenated copper, nickel-based alloys (Ni, Cr, Mo) — Alloy 22, Alloy C-4 (Hastelloy C4), etc., titanium alloys (including those with micro-additives of palladium, Ti 99.8 + Pd), zirconium (for example, Zircaloy), silicon carbide [4—11] and other materials are commonly considered as RW container materials.

Carbon steel-based materials are the most studied and have a number of obvious advantages over other EBS materials, including: a good combination of strength and ductility; generally satisfactory corrosion resistance; relative predictability of corrosion behavior. Moreover, they are mostly prone to areal rather than pitting (as opposed to stainless steels) corrosion. Extensive hands-on experience in the manufacturing and sealing of large cylindrical objects and low material costs are also seen as important advantages of this material.

Iron and carbon steel are metals that are unstable in acidic and neutral environments [12]. In an acidic medium, the highest corrosion rate is observed up to pH = 4, while at pH from 4 to 10 it remains approximately constant at a level of 0.1—1.0 μm/year.

In addition, the steel surface can undergo corrosion, which can also result from microbiological impacts associated with the microorganisms present both in the geological environment and the barrier materials. Many countries pay great attention to microbial or microbial-induced corrosion under relevant R&D programs focused on the processes occurring in geological repositories and aimed at safety demonstration [13, 14]. Microbial corrosion should be considered as a complex biogeochemical process. It can occur either due to the direct interaction of steel with cells, when iron or its chemical corrosion products act as electron donors in the processes of microbial respiration or it can be triggered by products of microbial metabolism, primarily hydrogen sulfide and organic acids [15]. [16] showed a twofold increase in the corrosion rate of steel in the presence of bacteria. [17] studied these processes with a focus placed on carbon steels under sterile and biotic conditions (in the presence of iron-reducing bacterium Shewanella oneidensis) at different temperatures under conditions similar to the underground RW disposal ones. It was found that in presence of bacteria, the corrosion rate of steel increased by 1.3—1.8 times. It was noted that in a chloride environment in the presence of various pure cultures, as well as in an environment with a mixed culture, the corrosion rate of API 5LX steel (0.22—0.26 % C, 0.9—1.2 % Mn), increased as compared to the one under sterile conditions with such an increase amounting to 3.1 times (from 0.95 to 2.95 mm/year) [18]. [19] studied the carbon steel 1018 corrosion under the thermophilic microbiota, including classical sulfate and iron reducers (*Geobacillus sp. G2, Bacillus sp. G9a, Bacillus sp. G11, and Desulfotomaculum sp. SRB-M*). A fourfold increase in the rate of its corrosion was observed in the presence of these bacteria; given a sterile setting, on the 25th day it amounted to (4.92 ± 4.90) g/m^2.

In terms of microbiological steel corrosion, sulfate-reducing bacteria (SRB) are considered as a most dangerous groups of microorganisms, which are viewed as common representatives of groundwater microflora [20—24]. Sulfate ions are required for their survival: they use them as an oxidizing agent in the processes of anaerobic respiration. Sulfate ions, being reduced to sulfide ions, result in increased corrosion-driven degradation rate of carbon steel in the presence of SRB. Oxygen resulting from the radiolysis under RW disposal conditions can also promote the development of thionic bacteria oxidizing sulfide ions to sulfate ions, with the latter ones, in turn, potentially stimulating the SRB growth. Thus, at the carbon steel — water interface, complex syntrophic oxidation-reduction processes of sulfur compounds can occur.

Temperature can have a contradictory effect on the biogeochemical process of steel corrosion. An increasing temperature can result in a decreasing chemical corrosion rate due to the formation of less soluble mineral phases (in contrast to corrosion product phases formed at lower temperatures) passivating the surface [26]. In case of a microbial process, temperature increase can result in the development of thermophilic or thermotolerant microbiota, which is likely to accelerate microbial corrosion. Environmental parameters play an important role in microbial processes, especially when it comes to biophilic elements required for a cell or an organic matter to survive. Upon steel interaction with clay barriers, the intensity of microbial processes can increase due to organic matter and biophilic elements present in clays [27]. However, bentonite material with a density of more than 1500—1900 kg/m^3 can significantly reduce the microbial activity [28—30].

This paper considers the corrosion of carbon steel grade St3 under sterile and non-sterile conditions simulating a deep RW disposal facility (DDF RW) at the Yeniseiskiy site. The study aims to develop an integrated corrosion model based on data from a series of experiments implemented both under sterile conditions and using the microbial community of samples taken from real-life objects.

Materials and methods

Under the experiments, carbon steel of grade St3 with its quality meeting the GOST 380-2005 standards [22]. The liquid phase, i. e., solutions simulating the groundwater of the Yeniseiskiy site, had the following composition: $NaHCO_3$ — 0.4 g/l, $MgSO_4 \cdot 7H_2O$ — 0.07 g/l, $CaCl_2$ — 0.075 g/l, pH = 7.0. Steel samples of 30 × 10 × 0.5 mm, previously prepared for the experiment (polished and defatted with alcohol) were weighed and emplaced into 10 ml of the liquid phase in hermetically sealed penicillin vials. In anaerobic experiments, argon was used as the gas phase with air applied as such under the aerobic experiments.

The experiment was implemented in triplicate for two weeks at temperatures of 20 and 50 °C. Microbiota samples were added by 1 ml (10 % of the original volume). Reference steel samples were those emplaced into the medium without any microbiota addition. The microbiota was collected from the water samples (depths of 30—40 m) and

cores (depths of 450—500 m) taken in the area of the Yeniseiskiy DDFRW site, as well as clay samples from the 10th Khutor deposit in Khakassia [31].

Corrosion behavior was evaluated via the gravimetric (gravimetric) method based on the measured changes in the mass of the samples during testing. After corrosion product removal, the specific weight loss was calculated using the following expression:

$$\frac{\Delta m}{S} = \frac{m_0 - m_1}{S}, \quad (1)$$

where m_0 is the mass of the sample before testing (g), m_1 is the mass of the sample after testing and removal of corrosion products and S is the area of the sample (m^2).

The data from this experiment served a basis for the corrosion model parameterization.

Carbon steel corrosion model

This study considers the kinetics equation for carbon steel areal corrosion depending on the properties of the medium:

$$V_{cor} = \frac{S \cdot \left(k_{an} + k_{aer} \cdot [O_2]\right) \cdot k_{bio} \cdot e^{-\frac{E_A}{RT}} \cdot \left(1 - SR(Fe_{met})\right)}{\left(1 + \sum_i k_1 \cdot EQ_{iPK}\right)^2} \quad (2)$$

where V_{cor} stands for corrosion rate of steel, mol/m^2·s (experimental study);
k_{aer} is the rate constant for the aerobic corrosion reaction, mol/m^2·s (calculated according to the experiments);
k_{an} is the rate constant for the anaerobic corrosion reaction, mol/m^2·s (calculated according to the experiments);
$[O_2]$ is the concentration of dissolved oxygen, mol/l;
k_{bio} is a constant accounting for biological effects (calculated according to the experiments);
E_A is the activation energy, J/mol (calculated according to the experiments);
R is the universal gas constant, J/mol·K;
T is the temperature,
S is the area of water contact with steel, m^2;
SR is the ratio of the current product of ion activities to a constant describing the reaction of iron dissolution;
k_1 are the coefficients calculated during the calibration of the model for the phases of ferrous and ferric iron;
EQ_{iPK} is the amount of the ith corrosion product, mol/l of water.

Model parameterization was done by comparing the experimental data with the model: the activation energy, the rate constant and the k_1 coefficient for the phases of ferrous and ferric iron were varied (2).

The calculation code for geochemical modeling PHREEQC 2.18 was used under the study [33]. The model allows the formation of the following corrosion products: siderite, iron II carbonate ($FeCO_3$), iron II and III hydroxides ($Fe(OH)_2$ and $Fe(OH)_3$) and iron II sulfide (pyrrhotite, FeS). The thermodynamic database *llnl.dat* was used, from which the forms of carbon, except for C(IV), were removed to exclude the formation of unrealistic oxidation degrees.

Corrosion rate of steel evaluated under laboratory conditions

Earlier evaluation focused on the composition of the microbial community present in groundwaters, soils (cores) and clays has revealed several groups of microorganisms important for the biocorrosion, which involve anaerobic sulfate-reducing and sulfide-oxidizing bacteria such as *Desulfomicrobium, Sulfuritalea, Desulfuromonas, Desulfovibrio, Thiobacillus,* bacteria with a fermentative type of metabolism forming organic acids and carbon dioxide and iron-oxidizing bacteria, capable of using metallic iron as an electron donor (representatives of the *Dechloromonas and Novosphingobium* genera). At elevated temperatures (50, 70, 90 °C), respiratory activity was recorded mainly in clay samples (at 50 and 70 °C). The presence of thermophilic or thermotolerant microorganisms should be considered in the forecasts regarding the safety of RW disposal facilities intended for RW Class 1, where significant heat release is expected due to radiation processes accompanied by the heating of the barrier system.

Under the experiments focused on the rate of microbial steel corrosion, studied was the role of various additives and their impact on this process. Figure 1 shows the appearance of carbon steel samples subject to corrosion under an experiment.

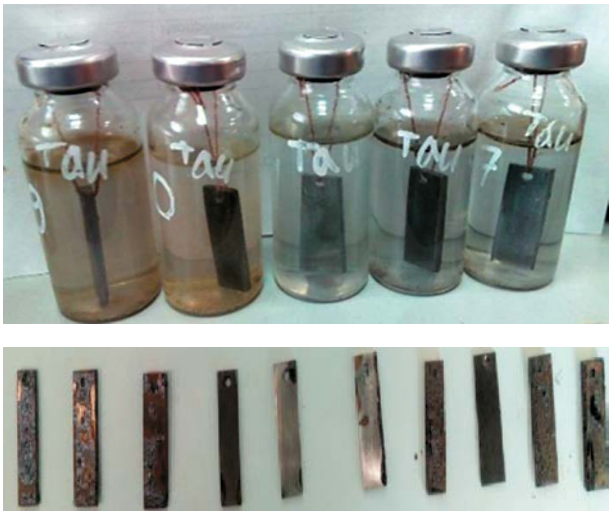

Figure 1. Appearance of ST3 steel samples subject to corrosion

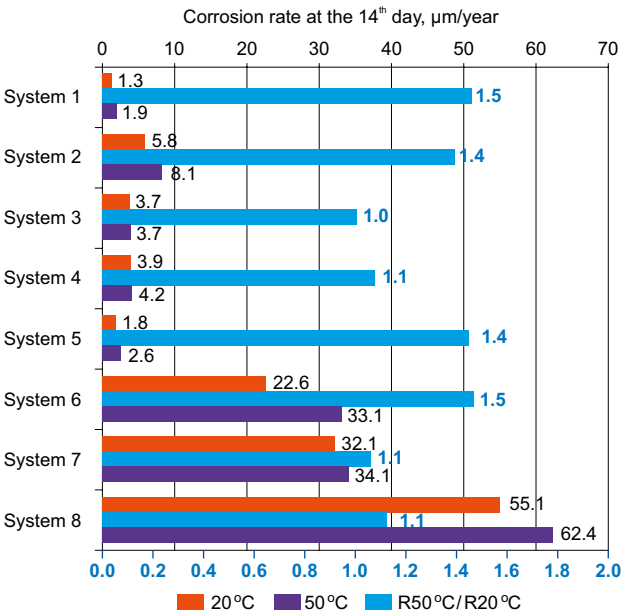

Figure 2. Corrosion rate of St3 steel (μm/year) at temperatures of 20 and 50° C under various conditions for 14 days

System 1 – sterile environment, anaerobic conditions;

System 2 – sterile environment, aerobic conditions;

System 3 – water from the Yeniseiskiy site, native microflora without additional stimulation, anaerobic conditions;

System 4 – water from the Yeniseiskiy site, native microflora, anaerobic stimulation in hydrogen;

System 5 – anaerobic environment, water from the Yeniseiskiy site, microbial community of the 10th Khutor brand bentonite;

System 6 – water from the Yeniseiskiy site, anaerobic stimulation with trehalose;

System 7 – water from the Yeniseiskiy site, anaerobic stimulation with sulfate (500 mg/l) and hydrogen;

System 8 – mixed microbial ground water communities from the Yeniseiskiy site and of the 10th Khutor brand bentonite, anaerobic stimulation with sulfate (500 mg/l) and hydrogen;

R_i – rate, μm/year, R50 °C / R20 °C – ratio of rates at temperatures of 50 and 20 °C (bottom axis)

Figure 2 shows the data on the corrosion rates for steel grade St3 resulted from a number of experiments implying various additives at temperatures of 20 and 50 °C.

It should be noted that, in general, under a temperature increase the corrosion rate increased by 10—20 %, which was indicating the presence of an active community with thermophilic or thermotolerant organisms capable of inducing the corrosion process. Experimental conditions 1—5 show a more realistic scenario for these processes. The average rate in model water typical for the Yeniseiskiy DDFRW conditions without microorganisms was up to 1.3—1.9 μm/year; in samples with real water taken from the site in the presence of microbiota under anaerobic conditions, it increased by 2—4 times staying below the level of 10 μm/year.

A most pessimistic corrosion scenario was observed in Systems 6 and 7 assuming the addition of organic matter, excess sulfate and hydrogen. Addition of trehalose (additive in System 6), which is a non-reducing chemically inert disaccharide, corrosion rate under aerobic and anaerobic conditions increased by 17 times. At the same time, it resulted in the release of metabolites contributing to an accelerated biocorrosion: carbon dioxide, anaerobic and organic acidic fermentation products. It is known that in bentonite clays the content of organic matter can reach 5 % potentially causing the intensification of microbial processes.

The corrosion rate was greatly influenced by the addition of sulfates with a concentration of 500 mg/l and hydrogen to the gas phase, which caused its increase to 34.1 μm/year. The presence of sulfates in the medium stimulated the growth of sulfate-reducing bacteria generating an aggressive metabolite — hydrogen sulfide, capable of binding with Fe^{2+} and reducing iron (III) hydroxide resulting in a dense iron sulfide precipitate. These processes generate galvanic pair iron (anode)—iron sulfide (cathode) accelerating the corrosion process.

The highest corrosion rate was observed in the sample of System 8 — up to 62.4 μm/year. In this case, microbial processes were accelerated due to the activation of a mixed microbial community of groundwaters and clays given the addition of sulfate and hydrogen, as well as organic matter and biophilic elements of clays, stimulating the growth of microorganisms. Thus, the synergistic effect of the mixed microbial community can significantly intensify steel corrosion processes.

It seems important to note that the calculated ratio of corrosion rates, R50 °C/R20 °C, at temperatures of 20 and 50 °C under sterile conditions was, as a rule, higher than in systems with biotically mediated corrosion (except for Systems 5 and 6) indicating the additivity of the biotic and abiotic corrosion processes. In this case, the rate of biologically mediated corrosion is either constant or changes little in a given temperature range. In this case, the contribution of abiotic oxidation processes is lower than the one of biotic processes (the corrosion rate in System 1 at temperatures of 20 and 50 °C were ranging from 1.3 to 1.9 μm/year).

Simulation of corrosion processes

Table 2 shows the model parametrization, i. e., the coefficients in equation (2), based on the experimental data from Table 1. Figure 3 compares relevant model and calculated indicators. Table 3 presents regression corrosion rate equations, as well as the forecasted corrosion rates, μm/year, at the 365th day given sterile conditions.

Table 1. Calculated corrosion rate given a sterile environment under anaerobic and aerobic conditions

Day	Corrosion rate, μm/year			Mean value	Std. dev.
	Experimental data				
	Max.	Intermediate	min.		
Anaerobic conditions					
Temperature 20 °C					
3	8.4	7.8	2.7	6.3	3.13
7	5.1	3.2	1.6	3.3	1.75
10	3.2	1.8	0.9	2.0	1.16
14	1.8	1.4	0.7	1.3	0.56
30	2	1	0.4	1.1	0.81
Temperature 50 °C					
3	12.3	7.6	5.7	8.5	3.40
7	5.3	2.8	2.1	3.4	1.68
10	2.8	2.6	1.8	2.4	0.53
14	2.6	1.7	1.3	1.9	0..67
30	1.8	1.7	0.6	1.4	0.67
Aerobic conditions					
Temperature 20 °C					
7	14.4	12.1	8.4	11.6	3.03
14	9.1	6.1	2.2	5.8	3.46
30	4.7	3.2	3.1	3.7	0.90
Temperature 50 °C					
7	18.9	14.6	13.2	15.6	2.97
14	12.6	8.8	2.9	8.1	4.89
30	8.9	5.2	3.3	5.8	2.85

Table 2. Parametrization of the model based on experimental data

Parameter in the equation (2)		Value
k_{aer}		0.924
k_{an}		$6.08 \cdot 10^{-5}$
k_1	$4.5 \cdot 10^3$	$4.5 \cdot 10^3$
	$2.8 \cdot 10^3$	$2.8 \cdot 10^3$
E_A	Anaerobic process	19 kJ/mol
	Aerobic process	21 kJ/mol
k_{bio}		4 – 17

Noteworthy is the fact that the activation energy of the anaerobic process calculated under this study work is lower than the literature value, which is 56 kJ/mol for anaerobic corrosion, according to [34]. Moreover, the coefficients calculated for the ferrous iron phases appeared to be higher than those for the trivalent iron, since the oxidation products of the latter one are looser and their generation passivates the surface to a lesser extent.

As can be seen from the results obtained, the model data are in fairly close agreement with the experimental data. One can note a minor discrepancy between the values predicted for the model and the extrapolation dependences. It should be emphasized that in aerobic model systems, transition from aerobic to anaerobic corrosion basically took place after the oxygen was exhausted (at the 71st day given a temperature of 50 °C and at the 121st day given a temperature of 20 °C). For this reason, the corrosion rate was recalculated given fully aerobic environment (the results are highlighted in brackets in bold type, Table 3).

Table 3. Regression corrosion rate equations and the predicted corrosion rate, μm/year at the 365th day given sterile conditions

System	Regression equation, R – rate, μm/year	R2	Rate according to the regress. eq., μm/year	Rate according to the chemical model at the 365th day, μm/year
Anaerobic corrosion				
20 °C, exper..	$R = 12.556\ [day]^{-0,703}$	0.927	0.20	0.23
20 °C, model	$R = 14.015\ [day]^{-0,799}$	0.995	0.13	
50 °C, exper.	$R = 17.695\ [day]^{-0,807}$	0.950	0.15	0.30
50 °C, model	$R = 15.713\ [day]^{-0,701}$	0.979	0.25	
Aerobic corrosion				
20 °C, exper.	$R = 51.448\ [day]^{-0,79}$	0.979	0.49	0.24 **(0.8)**
20 °C, model	$R = 50.631\ [day]^{-0,748}$ (**$R = 50.027\ [day]^{-0,747}$**)	0.992 (0.993)	0.61 **(0.61)**	
50 °C, exper.	$R = 54.253\ [day]^{-0,674}$	0.956	1.02	0.21 **(1)**
50 °C, model	$R = 58.501\ [day]^{-0,755}$ (**$R = 58.559\ [day]^{-0,753}$**)	0.990 (0.988)	0.69 **(0.75)**	

Under anaerobic corrosion conditions, the model showed iron sulfide and pyrrhotine generation, which demonstrates the realistic nature of the model itself: during the experimental study, blackening of steel samples was observed caused by sulfide phase the formation (Figure 3 displays this process and Figure 4 shows model accumulation of pyrrhotite). In addition, other compounds are formed under the corrosion process — magnetite or iron (III) hydroxide (given anaerobic corrosion conditions), iron (II) hydroxide and siderite (for aerobic corrosion conditions). In addition, other compounds are formed during the corrosion process — magnetite or iron (III) hydroxide (for anaerobic corrosion conditions), iron (II) hydroxide and siderite (under aerobic corrosion conditions).

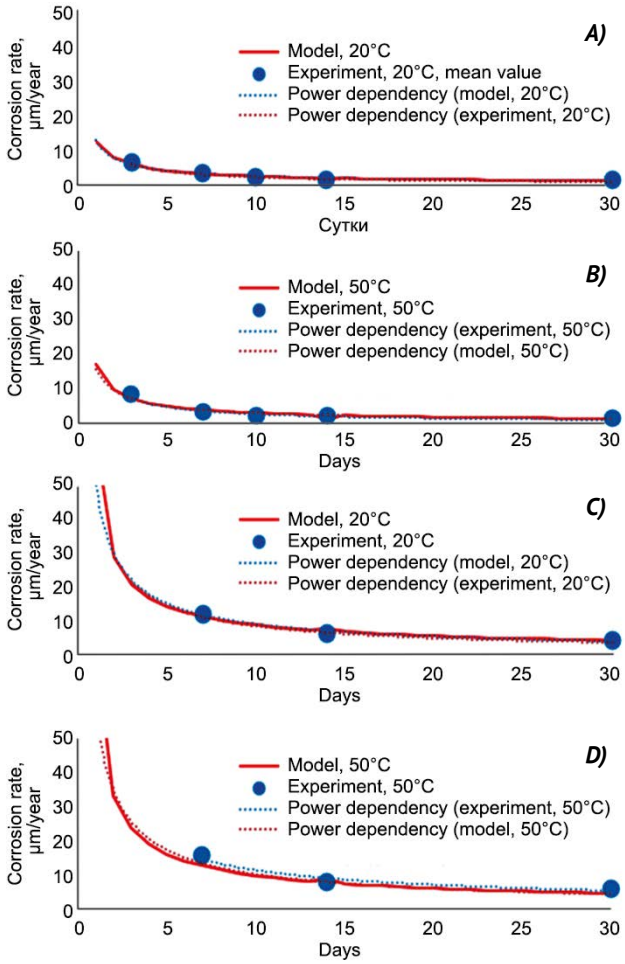

Figure 3. Comparison of model and calculated data on the corrosion rate under sterile conditions: A) anaerobic conditions, 20 °C; B) anaerobic conditions, 50 °C; C) aerobic conditions, 20 °C; D) aerobic conditions, 50 °C

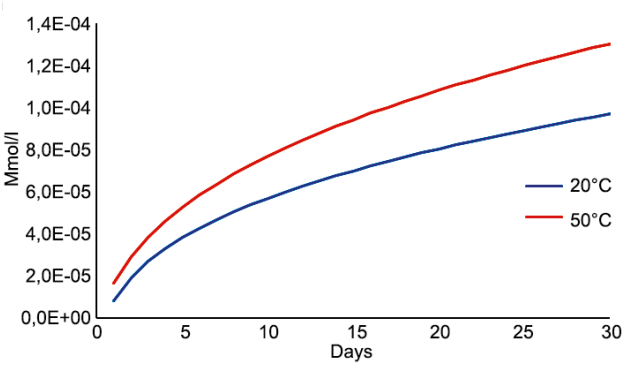

Figure 4. Model accumulation of pyrrhotite under steel sample corrosion in sterile experiments

Carbon steel corrosion rate forecasted based on the developed model

Figure 5 shows the calculated rate of areal anaerobic carbon steel corrosion assuming two conditions: with and without biogenic oxidation (according to a contribution similar to System 3). Since the temperature range of 20—50 °C was assumed under

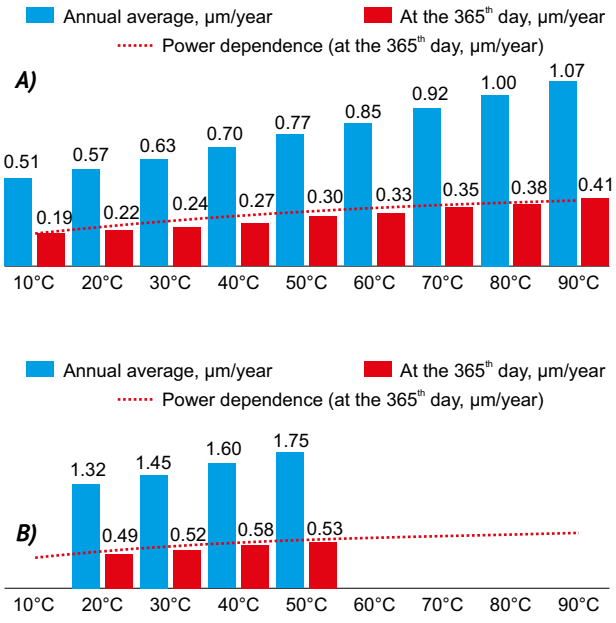

Figure 5. Calculated averaged time-dependent parameters referring to the rate of anaerobic areal carbon steel corrosion: A) no biogenic oxidation; B) with biogenic oxidation

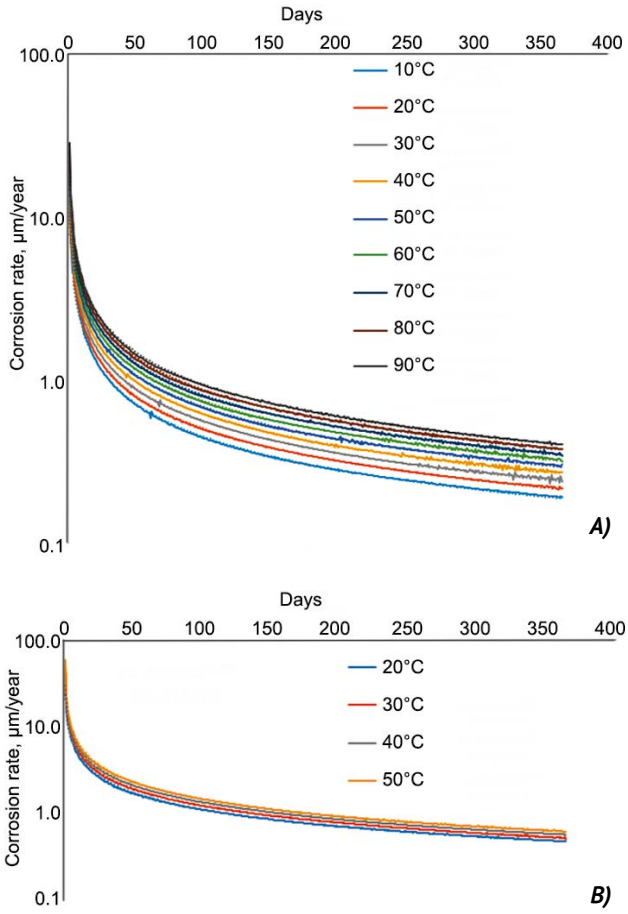

Figure 6. Calculated time-dependent corrosion rate of carbon steel: A) no biogenic oxidation; B) with biogenic oxidation

this experimental study of biogenic corrosion, biogenic contribution given other temperatures was not predicted.

Figure 6 shows the calculated rates of areal carbon steel corrosion as a function of assuming no biogenic oxidation. Table 4 presents the regression equations for the corrosion rate.

It can be noted that in the presence of bacteria, the rate of anaerobic oxidation becomes more similar to the one under aerobic corrosion conditions (see Table 3).

Table 4. Regression equations for the corrosion rate under anaerobic conditions

Temperature, °C	Regression equation, R — rate, μm/year	R2
No bacterial impact		
10	$R = 10.074\ [day]^{-0.675}$	0.9981
20	$R = 10.702\ [day]^{-0.662}$	0.9995
30	$R = 11.678\ [day]^{-0.658}$	0.9993
40	$R = 12.795\ [day]^{-0.656}$	0.9992
50	$R = 13.996\ [day]^{-0.655}$	0.9992
60	$R = 15.277\ [day]^{-0.655}$	0.9989
70	$R = 16.598\ [day]^{-0.655}$	0.9987
80	$R = 18.008\ [day]^{-0.656}$	0.9985
90	$R = 19.472\ [day]^{-0.658}$	0.9984
Given bacterial impact		
20	$R = 23.385\ [day]^{-0,657}$	0.9965
30	$R = 26.717\ [day]^{-0.664}$	0.9969
40	$R = 29.983\ [day]^{-0.669}$	0.9972
50	$R = 33.157\ [day]^{-0.672}$	0.9971

The calculated corrosion rates of steel presented in these figures, as well as the obtained regression equations can be used to estimate the corrosion rate under the disposal conditions at the Yeniseiskiy site assuming no contact with bentonite.

Conclusions

The paper focuses on the experimental study of microorganisms and their influence on the properties of steel safety barriers. The corrosion rate of carbon steel St3 samples was calculated considering both sterile conditions and the presence of a microbiological community sampled from the Yeniseiskiy site, as well as bentonite clays of 10th Khutor deposit. Corrosion rate in the presence of microorganisms turned out to be 2—30 times higher compared to the one characteristic for the abiotic corrosion process. It was found that temperature increase from 20 to 50 °C resulted in up to 1.5 times increase of the corrosion rate. A model has been developed accounting for chemical processes of oxidation and the formation of solid corrosion product phases, as well as the passivation of the steel surface with newly generated corrosion products.

References

1. NEA/EC. *Engineered Barrier Systems and the Safety of Deep Geological Repositories.* State-of-the-art Report, OECD Publishing, Paris, 2003.
2. Wang J. et al. The Beishan underground research laboratory for geological disposal of high-level radioactive waste in China: planning, site selection, site characterization and in situ tests. *Journal of Rock Mechanics and Geotechnical Engineering,* 2018, vol. 10, no. 3, pp. 411—435.
3. Dorofeev A. N., Bolshov L. A., Linge I. I., Utkin S. S., Saveleva E. A. Strategicheskii master-plan issledovanii v obosnovanie bezopasnosti sooruzheniya, ehkspluatatsii i zakrytiya punkta glubinnogo zakhoroneniya radioaktivnykh otkhodov [Strategic Master Plan for R&D Demonstrating the Safety of Construction, Operation and Closure of a Deep Geological Disposal Facility for Radioactive Waste]. *Radioaktivnye otkhody — Radioactive Waste,* 2017, no. 1, pp. 32—41.
4. Galtayries A., Marcus P., Terlain A., Desgranges C., Gauvain D., and Feron D. Oxidation of Materials for Nuclear Waste Containers Under Long Term Disposal. *Corrosion-2001, paper 01119.* NACE International, Houston, TX, 2001.
5. Smailos E. et al. *Corrosion studies on selected packaging materials for disposal of heat-generating radioactive wastes in rock-salt formations.* Final report 1991—1994. № FZKA-5587. Forschungszentrum Karlsruhe GmbH Technik und Umwelt (Germany). Inst. fuer Nukleare Entsorgungstechnik. Funding organisation: Commission of the European Communities, 1995.
6. Rebak R. B. *Selection of corrosion resistant materials for nuclear waste repositories.* No. UCRL-PRDC-221893. Yucca Mountain Project, Las Vegas, Nevada, 2006.
7. Vehovar L., Tandler M. Stainless steel containers for the storage of low and medium level radioactive waste. *Nuclear engineering and design,* 2001, vol. 206, no. 1, pp. 21—33.
8. Werme L. O. Fabrication and Testing of Copper Canister for Long-Term Isolation of Spent Nuclear Fuel. *MRS Online Proceedings Library,* 1999, vol. 608, no. 77. DOI: https://doi.org/10.1557/PROC-608-77.
9. Dunn D. S. et al. The localized corrosion resistance and mechanical properties of alloy 22 waste package outer containers. *JOM,* 2005, vol. 57, no. 1, pp. 49—55.

10. Druyts F., Kursten B. Influence of chloride ions on the pitting corrosion of candidate HLW overpack materials in synthetic oxidized boom clay water. *CORROSION-99*. OnePetro, 1999.
11. Babayants G. I. Ispol'zovanie karbida kremniya dlya sozdaniya penalov dlya dolgovremennogo khraneniya i zakhoroneniya VAO i OYAT [Application of Silicon Carbide in the Production of Canisters for Long-term Storage and Disposal of HLW and SNF]. *Bezopasnost' yadernykh tekhnologii i okruzhayushchei sredy — Nuclear Technology and Environmental Safety,* 2013.
12. DOE-DP-STD-3016-99. DOE Limited Standard. Hazard analysis reports for nuclear explosive operations. 1999.
13. Beech I. B, Sunner J. A, Hiraoka K. Microbe-Surface Interactions in Biofouling and Biocorrosion Processes. *Int. Microbiol.,* 2005, no. 8, pp. 157—168.
14. Lewandowski Z, Beyenal H. Mechanisms of Microbially Influenced Corrosion. In: Flemming H. C., Murthy P. S., Venkatesan R., Cooksey K. (eds) Marine and Industrial Biofouling. *Springer Series on Biofilms,* vol. 4. Springer, Berlin, Heidelberg. DOI: https://doi.org/10.1007/978-3-540-69796-1_3.
15. Kip N., van Veen J. The dual role of microbes in corrosion. *The ISME Journal: Multidisciplinary Journal of Microbial Ecology,* 2015, vol. 9, no. 3, pp. 542—551. DOI: https://doi.org/10.1038/ismej.2014.169.
16. Schütz M. K., Schlegel M. L., Libert M., Bildstein O. Impact of iron-reducing bacteria on the corrosion rate of carbon steel under simulated geological disposal conditions. *Environ. Sci. Technol.,* 2015, vol. 49, no. 12, pp. 7483—7490.
17. Schütz M. K., Schlegel M. L., Libert M., Bildstein O. Impact of iron-reducing bacteria on the corrosion rate of carbon steel under simulated geological disposal conditions. *Environ. Sci. Technol.,* 2015, vol. 49, no. 12, pp. 7483—7490.
18. Elumalai P. et al. Influence of thermophilic bacteria on corrosion of carbon steel in hyper chloride environment. *International Journal of Environmental Research,* 2017, vol. 11, no. 3, pp. 339—347.
19. Valencia-Cantero E., Peña-Cabriales J. J. Effects of Iron-Reducing Bacteria on Carbon Steel Corrosion Induced by Thermophilic Sulfate-Reducing Consortia. *J. Microbiology and Biotechnology,* 2014, vol. 24, no. 2, pp. 280—286.
20. El H. H. et al. Microbial corrosion of P235GH steel under geological condition. *Physics and Chemistry of the Earth,* 2010, vol. 35, pp. 248—253.
21. Féron D., Crusset D. Microbial induced corrosion in French concept of nuclear waste underground disposal. *Corrosion Engineering Science and Technology,* 2014, vol. 49, no. 6, pp. 540—547.
22. Venzlaff H., Srinivasan J., Mayrhofer K. J. J. et al. Accelerated cathodic reaction in microbial corrosion of iron due to direct electron uptake by sulfate-reducing bacteria. *Corrosion Science,* 2013, vol. 66, pp. 88—96. DOI 10.1016/j.corsci.2012.09.006.
23. Abdullah A. et al. Microbial corrosion of API 5L X-70 carbon steel by ATCC 7757 and consortium of sulfate-reducing bacteria. *Journal of Chemistry,* 2014, vol. 2014, pp. 1—7. DOI:10.1155/2014/130345.
24. Xu C. et al. Localized corrosion behavior of 316L stainless steel in the presence of sulfate-reducing and iron-oxidizing bacteria. *Materials Science and Engineering: A,* 2007, vol. 443, no. 1—2, pp. 235—241.
25. Ismail M., Noor N. Md., Yahaya N. et al. The Effect of pH and Temperature on Corrosion of Steel Subject To Sulphate-Reducing Bacteria. *Journal of Environmental Science and Technology,* 2014, vol. 7, iss. 4, pp. 209—217. DOI:10.3923/jest.2014.209.217.
26. Jullien M., Raynal J., Kohler É., Bildstein O. Physicochemical Reactivity in Clay-Rich Materials: Tools for Safety Assessment. *Oil and Gas Science and Technology,* 2005, vol. 60, pp. 107—120. DOI: 10.2516/ogst:2005007.
27. Marshall M. H. M. et al. Characterization of natural organic matter in bentonite clays for potential use in deep geological repositories for used nuclear fuel. *Applied Geochemistry,* 2015, vol. 54, pp. 43—53.
28. Pusch R. Mobility and survival of sulphate-reducing bacteria in compacted and fully water saturated bentonite — microstructural aspects. SKB TR-99-30. Svensk Kärnbränslehantering AB, 1999.
29. Pedersen K. Microbial processes in radioactive waste disposal. SKB TR-00-04. Svensk Kärnbränslehantering AB, 2000.
30. Stroes-Gascoyne S., Hamon C. J., Dixon D. A. The effects of dry density and porewater salinity on the physical and microbiological characteristics of highly compacted bentonite. Ontario Power Generation Report No. 06819-REP-01200-10016-R00, 2006.
31. Belousov P. E. et al. Bentonite clays from 10th Khutor deposite: features of genesis, composition and adsorption properties. *RUDN Journal of Engineering Researches,* 2017, vol. 18, no. 1, pp. 135—143.
32. GOST 380-2005. *Mezhgosudarstvennyi standart. Stal' uglerodistaya obyknovennogo kachestva* [Interstate Standard. Carbon Steel of Ordinary Quality].
33. Parkhurst D. L. et al. User's guide to PHREEQC (Version 2): A computer program for speciation, batch-reaction, one-dimensional transport, and inverse geochemical calculations. *Water-resources investigations report,* 1999, vol. 99, no. 4259, pp. 312.
34. *A Survey of Steel and Zircaloy Corrosion Data for Use in the SMOGG Gas Generation Model.* Report to the NDA RWMD. SA/ENV-0841. Issue 3. 2010.

Information about the authors

Boldyrev Kirill Aleksandrovich, Candidate of Technical Sciences, Senior Researcher, Nuclear Safety Institute of the Russian Academy of Sciences (52, Bolshaya Tulskaya st., Moscow, 115191, Russia), e-mail: kaboldyrev@ibrae.ac.ru.

Safonov Aleksej Vladimirovich, Candidate of Chemical Sciences, Leading Researcher, Federal State Budgetary Institution of Science A. N. Frumkin Institute of Physical chemistry and Electrochemistry of the Russian Academy of Sciences (31, bld.4, Leninsky prospect, Moscow, 119071, Russia); Nuclear Safety Institute of the Russian Academy of Sciences (52, Bolshaya Tulskaya st., Moscow, 115191, Russia), e-mail: alexeysafonof@gmail.com.

Abramova Elena Sergeevna, engineer, Federal State Budgetary Institution of Science A. N. Frumkin Institute of Physical chemistry and Electrochemistry of the Russian Academy of Sciences (31, bld.4, Leninsky prospect, Moscow, 119071, Russia), e-mail: gorchicta246@mail.ru.

Gladkikh Natalya Andreevna, Candidate of Chemical Sciences, Senior Researcher, Federal State Budgetary Institution of Science A. N. Frumkin Institute of Physical chemistry and Electrochemistry of the Russian Academy of Sciences (31, bld.4, Leninsky prospect, Moscow, 119071, Russia), e-mail: fuchsia32@bk.ru.

Kryuchkov Dmitry Vyacheslavovich, Candidate of Technical Sciences, Head of the Laboratory, Nuclear Safety Institute of the Russian Academy of Sciences (52, Bolshaya Tulskaya st., Moscow, 115191, Russia), e-mail: dvk@ibrae.ac.ru.

Bibliographic description

Boldyrev K. A., Safonov A. V., Abramova E. S., Gladkikh N. A., Kryuchkov D. V. Research on the St3 Carbon Steel Corrosion in the Presence of Microorganisms Isolated from the Groundwater at the Yeniseyskiy Site. *Radioactive Waste,* 2021, no. 3 (16), pp. 103—113. DOI: 10.25283/2587-9707-2021-3-103-113. (In Russian).